IMPEDANCE AND SINGLE-BUNCH INSTABILITIES IN THE ILC DAMPING RING.*

M. Korostelev[†], A. Thorley, A. Wolski, University of Liverpool and the Cockcroft Institute, UK
N. Collomb, J. Lucas, S. Postlethwaite, STFC Technology, Daresbury Laboratory, UK
O. B. Malyshev, STFC ASTeC, Daresbury Laboratory, UK

Abstract

The longitudinal wake fields have been calculated by using a 3D electromagnetics code, CST Particle Studio, for a number of different vacuum chamber components in the 6.4 km ILC damping ring. Studies of bunch lengthening and single-bunch instabilities have been carried out. Bunch lengthening from a particle tracking code are compared with results from numerical solution of the Haissinski equation. The tracking code is used to predict the threshold for single-bunch instabilities.

INTRODUCTION

Short-range wake fields in a storage ring can lead to distortion of the longitudinal phase space distribution and single-bunch instabilities. The instability threshold (expressed in terms of the bunch charge) depends on the lattice parameters and the geometry of the vacuum chamber.

The latest lattice design for the ILC damping rings (DCO4 [1]) provides good flexibility in variation of momentum compaction factor over a range from 2.9×10^{-4} to 1.3×10^{-4}, by tuning the horizontal phase advance per arc cell over a range from $72°$ to $100°$. The RF voltage is adjusted to maintain the specified bunch length of 6 mm rms over this range. The lattice has a racetrack layout with circumference of 6476.4 m, and a beam energy of 5 GeV. The arcs include 200 dipoles. A series of 88 superconducting wiggler magnets is located in one of the two long straight sections. The precise value of the circumference is chosen to accommodate a range of fill patterns, from 2610 bunches with a bunch population of 2×10^{10} particles, to 5265 bunches with a bunch population of 1×10^{10}.

The mechanical and vacuum design for the arc and wiggler section has now been developed [2]. The vacuum chamber of the damping ring mostly consists of straight cylindrical aluminium tubes with inner diameter of 58 mm. There is a rectangular slot (antechamber) on one side in each arc dipole, and an antechamber on both sides of the cylindrical vacuum chamber in the wiggler magnet. A synchrotron radiation power absorber with complex tapered geometry is inserted just after each wiggler. All button type beam position monitors (BPMs) are connected to the vacuum chamber through bellows and multi-strip RF shielding, forming so-called BPM insertions. There are 692 BPMs in total in the ring.

WAKE FIELD CALCULATIONS

The longitudinal wake potentials (monopole wake field component) for the BPM insertions, absorbers, and antechamber tapers were computed using CST Particle Studio [3]. An ultra-relativistic bunch with length of 6 mm rms is used as a source of excitation. Open boundary conditions are assigned at the entrance and exit of the structure to be modelled. Wake field analysis shows that the smooth tapers from the antechamber to the circular profile main vacuum chambers in the arcs and wigglers produce relatively small wake potentials compared with the BPM insertions and absorbers. Since the overall number of the antechamber tapers is smaller than the total number of BPMs and absorbers, we do not consider their contribution to the wake field within the scope of this paper.

The BPM insertion [4] is 40 cm long, with a volume of $4070 \, \text{cm}^3$ under vacuum. A high resolution hexagonal mesh is required for accurate discretization of many complex details with sizes < 1 mm. Figure 1 shows the longitudinal wake potentials of the BPM insertion computed over a distance of 1 m at 26 lines per wavelength (in terms of CST parameters), but with two different constraints for the maximum longitudinal mesh step: the grey and blue wake potentials correspond to a maximum longitudinal mesh step of 0.17 mm (150 million mesh cells per quarter of the 3D structure) and 0.1 mm (250 million mesh cells per quarter of the 3D structure), respectively. As expected, a mesh with a smaller longitudinal step results in a better accuracy for the wake field solution: in particu-
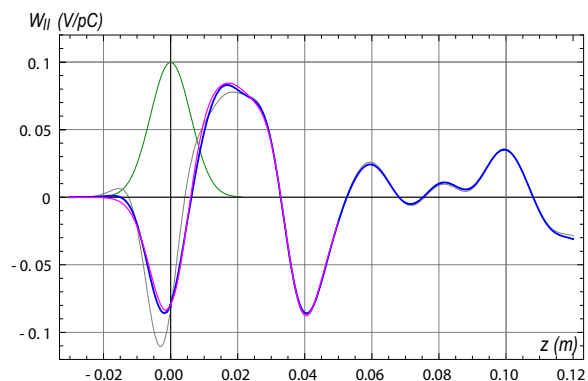

Figure 1: Longitudinal wake potentials of BPM insertion computed by CST (blue and grey lines); wake potential convoluted from the wake function (magenta line); normalized charge density of the bunch (green line).
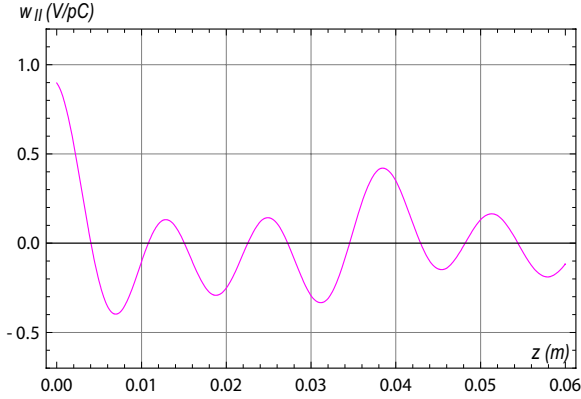
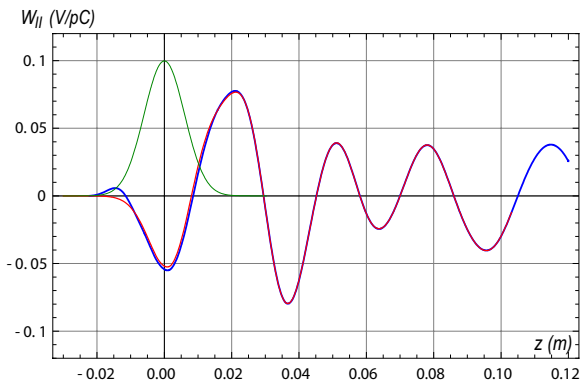Figure 2: Longitudinal wake function of the BPM insertion.

Figure 3: Longitudinal wake potentials of the absorber computed by CST (blue line); wake potential convoluted from the wake function (red line); normalized charge density of the bunch (green line).
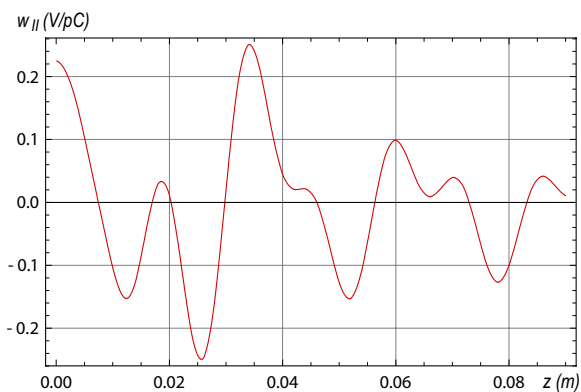

Figure 4: Longitudinal wake function of the absorber.

lar, there is a significant reduction in the unphysical wake occurring ahead of the bunch. The beam loss factor produced by one BPM insertion is 0.043 V/pC, where the BPM buttons contribute only 0.007 V/pC. At the nominal beam current of 400 mA, the average dissipated power per BPM insertion would be 53 W.

The wake function shown in Fig. 2 is obtained from the longitudinal wake potential. The wake potentials computed directly by CST are compared with the wake potentials evaluated as a convolution of the charge distribution and the wake function: the results are in good agreement, as shown in Fig. 1, indicating that the wake function has been computed with reasonable accuracy.

The absorber has two-fold symmetry with ramped surface geometry on each side, and circular aperture that tapers from 52 mm internal diameter to 44 mm internal diameter, to provide shadowing of downstream components from synchrotron radiation [2]. Figure 3 shows the longitudinal wake potential computed for the absorber. The corresponding wake function is shown in Fig. 4, while its convolution with the charge distribution is shown in Fig. 3 (red line). The beam loss factor and average dissipated power per absorber are 0.03 V/pC and 37 W, respectively. There is a small unphysical wake ahead of the bunch: this is likely the result of non-uniform cross-sections at the entrance and exit of the structure and mesh resolution.

INSTABILITY THRESHOLD

The single-bunch instability threshold has been computed using a parallel tracking code. The code evolves the longitudinal phase space distribution turn by turn taking into account the RF cavities, the momentum compaction, synchrotron radiation damping and excitation, and longitudinal wake fields. The bunch charge distribution is represented by a number of point-like macroparticles with equal charge. The change in the energy deviation of each macroparticle resulting from the wake field is computed from the convolution of the wake function and macroparticle charge distribution. Macroparticle tracking running in parallel on a multi-core GPU results in a performance increase approximately $60\times$ over the sequential processing of an equivalent code running on a CPU.

The wake functions obtained from CST Particle Studio are used in our study as input data for the code. The evolution of the longitudinal phase space distribution is computed over 2,500 turns (just over 5 longitudinal damping times) with 2^{19} macroparticles per bunch. For bunch populations below the instability threshold, radiation effects lead to the distribution reaching equilibrium. For fixed RF voltage, we observe a steady increase in the equilibrium rms bunch length as a function of bunch population (potential well distortion); the rms energy spread remains roughly constant up to the instability threshold, at which point it rises rapidly.

Figure 5 shows the results of tracking in the lattice with arc cell phase advance of $100°$ (momentum compaction factor of 1.3×10^{-4}). The circles correspond to the wake field generated by 692 BPM insertions only while the crosses represent the wake field generated by 692 BPM insertions and 88 absorbers. From the point at which the energy spread starts to increase, we identify the instability threshold as $\sim 33 \times 10^{10}$ particles per bunch in the presence of the BPM wake field only. Including the wake
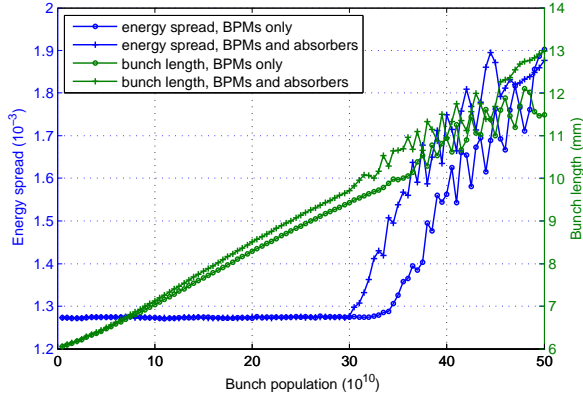
Figure 5: Evolution of rms energy spread and rms bunch length with bunch population in the case of $100°$ per arc cell.
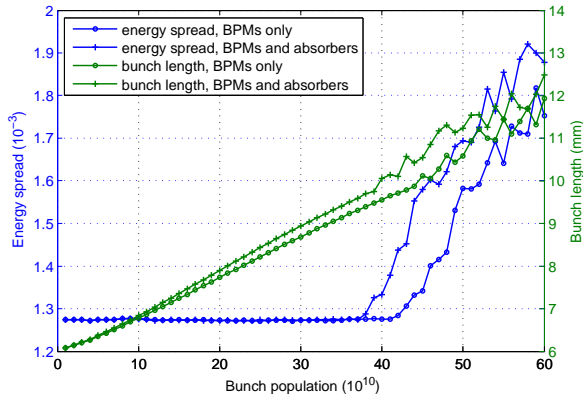

Figure 6: Evolution of rms energy spread and rms bunch length with bunch population in the case of $90°$ per arc cell.

field from the absorbers reduces the instability threshold to $\sim 30 \times 10^{10}$ particles per bunch; however, the threshold is still far from the maximum bunch population of 2×10^{10} specified for the damping ring.

Based on the bunch population at which an instability occurs, an effective value for the broad-band impedance $|Z/n|$ may be estimated from the Keil-Schnell-Boussard criterion. In the case that only the BPM insertions are included, the effective value of $|Z/n|$ is $10\,\text{m}\Omega$; this rises to $12\,\text{m}\Omega$ if the absorbers are included. If we scale the impedance at which an instability occurs with the bunch population and bunch length, then to remain below the instability threshold for the nominal maximum bunch population of 2×10^{10} particles, the effective broad-band impedance should not exceed $235\,\text{m}\Omega$, $130\,\text{m}\Omega$ and $105\,\text{m}\Omega$ for the lattices with arc cells tuned to $72°$, $90°$ and $100°$ phase advance, respectively.

Figure 6 shows the results of the tracking simulation for the lattice with phase advance $90°$ per arc cell (momentum compaction factor of 1.6×10^{-4}). Tuning the arc cells to lower phase advance increases momentum compaction
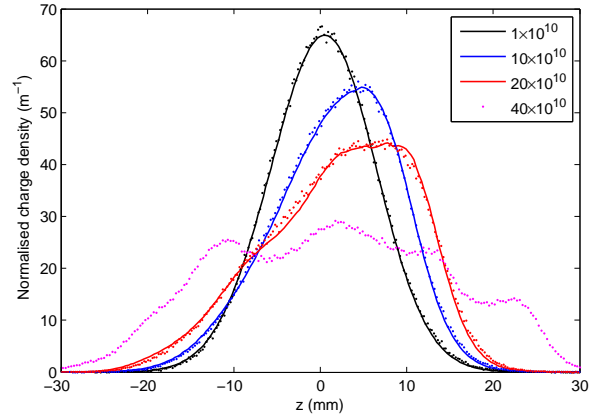

Figure 7: Variation of longitudinal charge distribution with bunch population in presence of wake files generated by all BPM insertions and absorbers. Points represent the results of a tracking simulation, lines show the solution of the Haissinski equation. Arc cell phase advance is $100°$.

factor, and raises the instability threshold.

Below the instability threshold, the results of the tracking simulation for the longitudinal charge distribution are in a very good agreement with the solution of the Haissinski equation [5], as shown in Fig. 7. The solutions to the Haissinski equation are found using a numerical iterative technique.

CONCLUSION

3D computations of the longitudinal wake field have been performed for BPM insertions and synchrotron radiation absorbers in the DCO4 ILC damping ring lattice. A parallel tracking code has been developed for studies of bunch lengthening and single-bunch instability. Below instability threshold, the longitudinal distributions found from the tracking simulations are in very good agreement with analytical predictions from the Haissinski equation. The lowest instability threshold is more than an order of magnitude larger than the bunch population specified for the damping ring: this provides a good margin for the impedance of additional components, including RF cavities, kickers, etc.

REFERENCES

[1] M. Korostelev and A. Wolski, "Lattice design for the 6.4 km ILC damping rings," these proceedings (IPAC'10).

[2] O.B. Malyshev, J.M. Lucas, N. Collomb, S. Postlethwaite et al., "Mechanical and vacuum design of wiggler section of ILC DR," these proceedings (IPAC'10).

[3] Computer Simulation Technology, http://www.cst.com/

[4] M. Korostelev, A. Wolski, "Wake field simulations for the vacuum chamber transitions of the ILC damping ring," (PAC'09).

[5] J. Haissinski, Nuovo Cimento 18B, 72 (1973).